

Force Statistics and Wake Structure Mechanism of Flow around a Square Cylinder at Low Reynolds Numbers

Shams-Ul-Islam, Waqas Sarwar Abbasi, Hamid Rahman

Abstract—Numerical investigation of flow around a square cylinder are presented using the multi-relaxation-time lattice Boltzmann methods at different Reynolds numbers. A detail analysis are given in terms of time-trace analysis of drag and lift coefficients, power spectra analysis of lift coefficient, vorticity contours visualizations, streamlines and phase diagrams. A number of physical quantities mean drag coefficient, drag coefficient, Strouhal number and root-mean-square values of drag and lift coefficients are calculated and compared with the well resolved experimental data and numerical results available in open literature. The Reynolds numbers affected the physical quantities.

Keywords—Code validation, Force statistics, Multi-relaxation-time lattice Boltzmann method, Reynolds numbers, Square cylinder.

I. INTRODUCTION

THE vortex shedding and force statistics from bluff bodies is an important engineering studied problem. The vortex shedding and force statistics strongly depend upon the cylinder size, computational domain and Reynolds numbers. Furthermore, the analysis of shed vortices behind the bluff body is another challenging task. Experimentally to investigate all the above mentioned aspects are extremely difficult especially at low Reynolds numbers (Re). Due to advancement of numerical methods and development of computer technology one can easily investigate all the aspects. Furthermore, using the newly developed numerical methods the code validation is very important before dealing with complex problems. The vortex-shedding frequencies, pressure distribution, lift, drag, Strouhal numbers and onset of vortex shedding for flow past a square cylinder were studied experimentally by mostly Okajima [1], Davis and Moore [2], Norberg [3] and Dutta et al. [4]. Whereas Sohankar et al. [5], Robichuax et al. [6], De and Dalal [7], Gera et al. [8] and Alshayji and Abograis [9] have worked numerically on different aspect for flow past a square cylinder.

Okajima [1] experimentally examined the vortex-shedding frequencies of various rectangular cylinders by using a wind tunnel and water tank. He found that a certain range of Reynolds numbers for cylinders with width-to-height ratios of 2 and 3 exist where the flow pattern showing a sudden

discontinuity in the Strouhal number. Davis and Moore [2] experimentally and numerically studied the two-dimensional time-dependent flow for Reynolds numbers ranging between 100 and 2800. They observed that the shed vortices, lift, drag and Strouhal number strongly dependent on Reynolds numbers. Norberg [3] experimentally investigated the flow and pressure around rectangular cylinders at different angle of attack. He also examined the side ratios effect and measured the static pressure distribution. He examined the Strouhal number for associated wake frequencies by using the hot wire measurements. He found multiple wake frequencies for some Reynolds numbers for side ratios ranging between 2 and 3. Dutta et al. [4] experimentally measured the low Reynolds numbers between 97 and 187 for flow past a square cylinder by using hotwire anemometry. They found that vorticity decays faster at low Reynolds numbers in the downstream direction as compared to high Reynolds numbers. Furthermore, at high Reynolds numbers, the magnitudes of the vorticity decrease with distance. Sohankar et al. [5] numerically calculated the force coefficients for flow past a square cylinder at different Reynolds numbers using the SIMPLEC finite volume code and third-order QUICK scheme. They also examined the effect of inflow location, outflow location and side wall locations at $Re = 100$. They found that the onset of vortex shedding occurs between $Re = 50$ and 55. Robichuax et al. [6] numerically investigated the onset of three-dimensionality for flow past a square cylinder and observed that the transition process is similar to that of a circular cylinder.

The present work is basically motivated to provide a systematic code validation study by using the lattice Boltzmann method in terms of all aspects and also to provide a detail comparison with existing experimental data and numerical results in open literature for future analysis. In this paper we mainly focused on the multi-relaxation-time lattice Boltzmann method and the numerical data for physical parameters using the single-relaxation-time lattice Boltzmann method also given in this study for comparison. One can easily find the details of multi-relaxation-time lattice Boltzmann method (MRT-LBM) together with the initial and boundary conditions in Shams et al. [10]. Shams et al. [10] systematically discusses the effect of the computational domain on the flow past a square cylinder in detail in terms of vorticity contours visualization and physical parameters with experimental and numerical comparison. Furthermore, they also given the detail problem description and important

Shams-Ul-Islam is with the Mathematics Department, COMSATS Institute of Information Technology Islamabad, 44000, Pakistan (corresponding author, Phone: 0092-3139840066; e-mail: islam_shams@comsats.edu.pk).

Waqas Sarwar Abbasi and Hamid Rahman are with the Mathematics Department, COMSATS Institute of Information Technology Islamabad, 44000, Pakistan (e-mail: waqas-555@hotmail.com, hamid_icp@yahoo.com).

physical parameters that we now used in this paper. The lattice Boltzmann equation (LBE) is a new numerical scheme originated from the lattice gas model (LGM) in order to overcome the main difficulties in LGM [11]. One can easily find the importance, theoretical background and applicability in practical engineering applications [12]-[24].

Before proceeding to results and discussion section, firstly, we will discuss the adequacy of the grid. The spatial adequacy was tested by varying the number of grid points (10, 20 and 40 points) representing a cylinder and comparing values of mean drag coefficient and Strouhal number for different Reynolds numbers (see Figs. 1 (a), (b)). The cylinder is placed d from the inlet position and the computational domain comprises 921×261 points for the 20-point grid in this evaluation. It is observed that the variation in mean drag coefficient and Strouhal number between the last two selected resolutions for chosen Reynolds numbers is small ($<2.3\%$). Furthermore, no significant variation observed in terms of Strouhal number. It is confirmed that the computations on the 20-points grid have converged for the selected parameters. It is important to state here that the percentage deviation relative to the 40 points calculated in this study for data presented in Figs. 1 (a), (b).

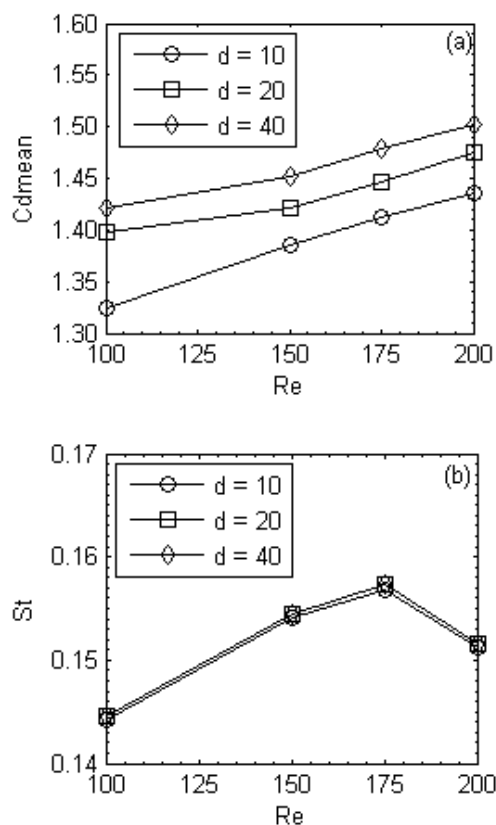


Fig. 1 Variation of (a) C_{dmean} and (b) St for different size of square cylinder

The rest of the paper is organized as follows: The effects of the Reynolds numbers on the physical quantities, vortex shedding frequencies and the flow structures are discussed in

Section II compared with experimental data and numerical results. Finally important findings are summarized in Section III.

II. RESULTS AND DISCUSSIONS

Numerical calculations were carried out for flow around a square cylinder for Reynolds numbers. The present calculations yield time series for the force coefficients, power spectra analysis of lift coefficient, vorticity contours visualization, streamlines and phase diagram for different combinations. Calculations of the mean drag coefficient (C_{dmean}), drag coefficient (C_d), Strouhal number (St), and root-mean-square values of drag ($C_{d rms}$) and lift ($C_{l rms}$) coefficients in terms of physical parameters for square cylinder are also given. It is important to mention here that we calculate the Strouhal number using the fast Fourier transform technique. In vorticity graphs the solid lines represent the positive vortices generated from the lower corner of the cylinder and dashed line presents the negative vortices generated from the upper corner. Moreover in drag coefficient, lift coefficient, Strouhal and phase graphs solid lines are used. It is also important to state here that those cases that they have similar characteristics are not shown in this paper and some representative cases will be discussed.

To analyze the effect of Reynolds number on vortex shedding, the vorticity contours visualizations are presented in Figs. 2 (a)-(f). It can be easily observed that the vortex shedding size and width behind the cylinder showing some changes by increasing the Reynolds number. At $Re = 80$, a positive vortex on the lower side of the cylinder appears and at the same time the negative vortex from the upper side of the cylinder is roll up (see Fig. 2 (a)). The vortex shedding process is almost similar to that observed for other Reynolds numbers. Furthermore, we observed that a negative vortex on the upper side of the cylinder is about to detach, while a positive vortex on the lower side of the cylinder in the development process (Figs. 2 (d)-(f)). Such kind of vortex shedding characteristics observed by Cheng et al. [18] for flow around a square cylinder in a uniform shear flow using the lattice Boltzmann method. We not observed the distortion and merging of shed vortices behind the cylinder for all selected Reynolds numbers in this study. This clearly indicates the capability of the present code for bluff body flows. One can clearly see the complete Karman vortex street behind the cylinder. The wake circulation length of the initially generated negative and positive shed vortices from the upper and lower side of the cylinder affected and reduced by increasing the Reynolds numbers, respectively. In addition, the mean position of the positive and negative vortices remains same throughout computational domain behind the square cylinder. This ensures that the separation point is same for all Reynolds numbers and also clearly seen in streamline graphs (see Figs. 3 (a)-(f)).

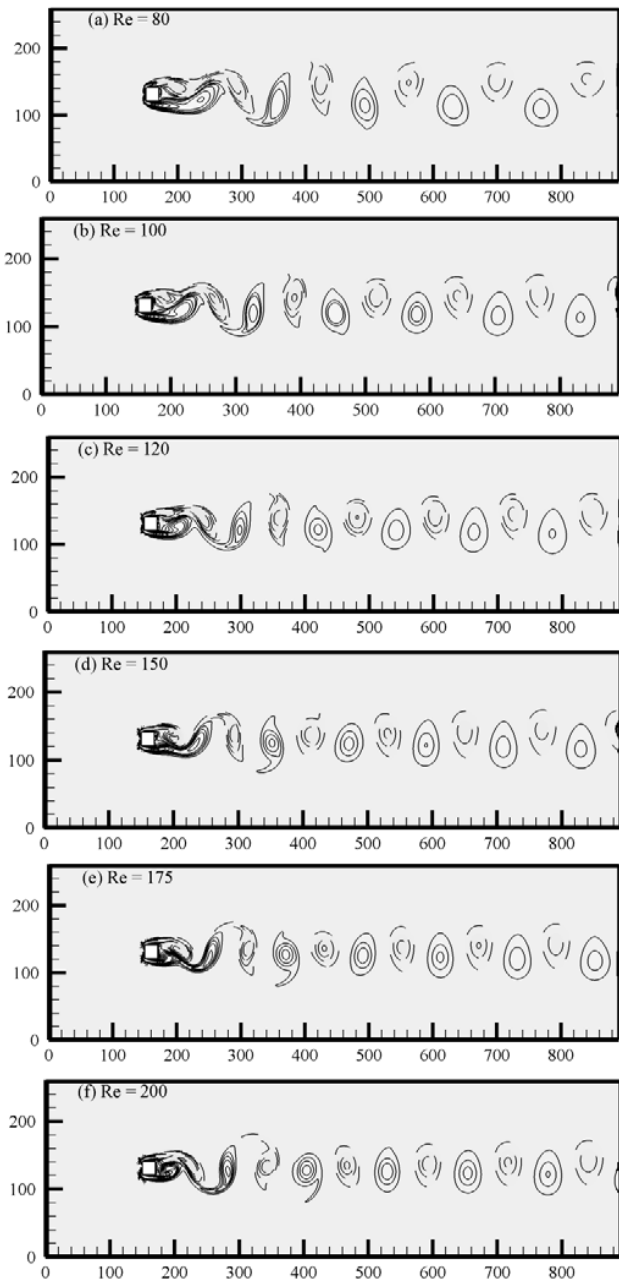


Fig. 2 (a)-(f) Vorticity contour plots at different Reynolds numbers

To further validate the code and to analyze the effect of Reynolds numbers on flow around a square cylinder streamline visualization are presented in Figs. 3 (a)-(f). It is clearly observed from streamlines that once the Reynolds numbers increased the shed vortices either appeared quickly from the upper side or lower side and then travel downstream without any merging and distortion. The separation point from the front surface is same for all selected Reynolds numbers. The stagnation point changes with Reynolds numbers for flow behind the square cylinder and even at the surface of the cylinder also.

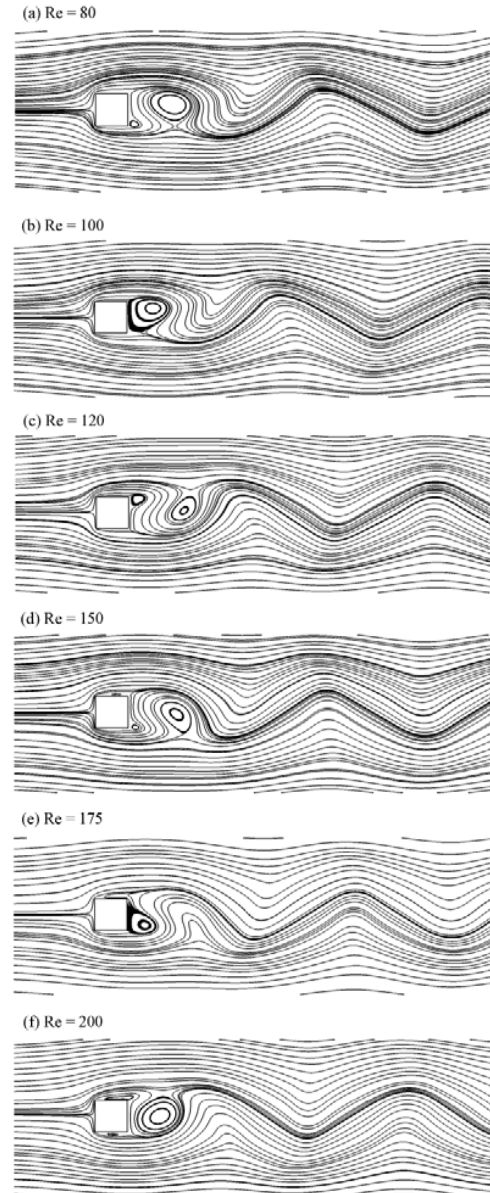


Fig. 3 (a)-(f) Streamline visualization of flow past a square cylinder at different Reynolds numbers

The time-trace analysis of drag and lift coefficients for some selected Reynolds numbers are shown in Figs. 4 (a)-(d) and 5 (a)-(d). The periodic natures in terms of drag and lift coefficients observed for all selected Reynolds numbers in this study. The amplitude of drag and lift coefficients either increased or decreased by increasing the Reynolds numbers. Davis and Moore [2] experimentally observed such kind of variation for lower and higher Reynolds numbers. The sinusoidal variation of lift coefficients (see Figs. 5 (a)-(d)) clearly indicates the fully developed Karman vortex street behind the square cylinder for all Reynolds numbers without any merging and distortion throughout the computational domain in this study.

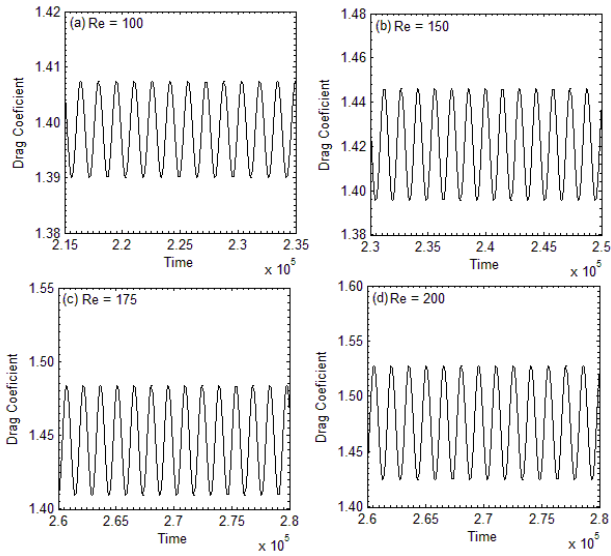


Fig. 4 (a)-(d) Time-trace analysis of drag coefficients for some selected Reynolds numbers

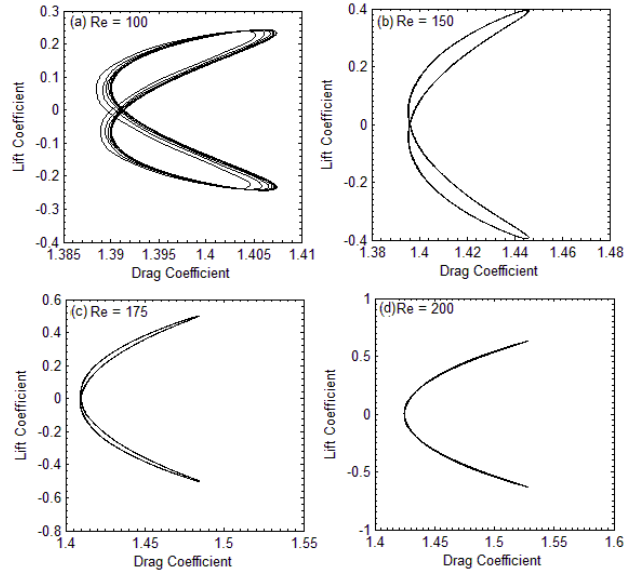


Fig. 6 (a)-(d) Phase diagram of drag and lift coefficients for some selected Reynolds numbers

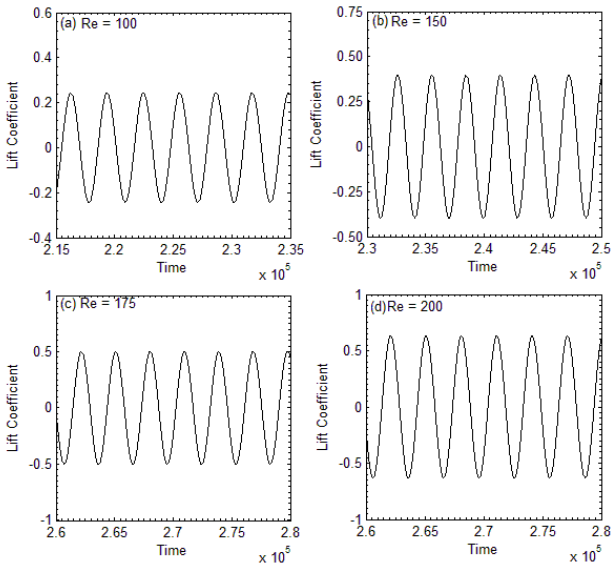


Fig. 5 (a)-(d) Time-history analysis of lift coefficients for some selected Reynolds numbers

The phase diagram of drag and lift coefficients are shown in Figs. 6 (a)-(d) for some selected Reynolds numbers. The eight phase figure observed for all Reynolds numbers. In Figs. 6 (a)-(d), one can also see that the mean position of the drag and lift coefficients is zero. This means that the separation point of vortices remains same for all chosen Reynolds numbers. The phase diagram clearly shows the variation in drag and lift coefficients and the shed vortices size and width by increasing the Reynolds numbers. Again this ensures that the present code can capture the complex flow phenomenon easily.

The power spectrum analysis of lift coefficients is presented in Figs. 7 (a)-(d). The amplitude of the spectrum energy increase by increasing the Reynolds numbers. The single peak observed in the spectrum which is the primary vortex shedding frequency. No secondary cylinder interaction frequency observed in this study. This means that one can easily capture the fully developed vortex street behind the cylinder up to Reynolds number 200 using the multi-relaxation-time lattice Boltzmann method. This ensures again the applicability and validity of the present code.

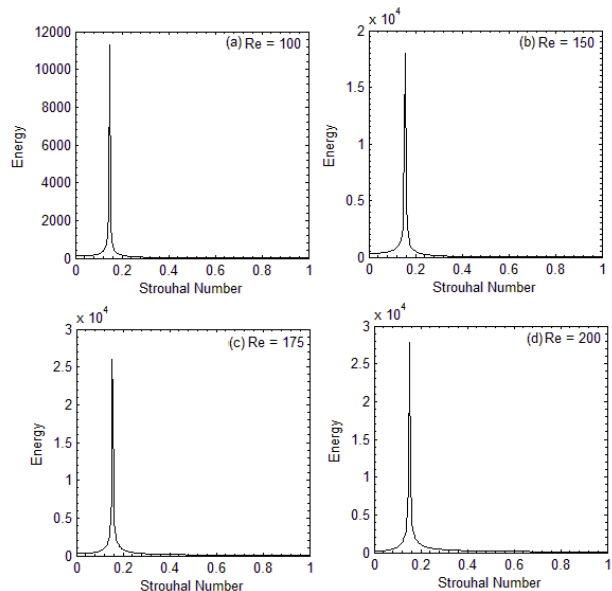


Fig. 7 (a)-(d) Power spectrum analysis of lift coefficients at different Reynolds numbers

The variation of mean drag coefficient (C_{dmean}), drag coefficient (C_d) and Strouhal number (St) for different Reynolds numbers are shown in Figs. 8 (a), (b). It is important to state here that C_d means the highest peak in drag coefficient amplitude (see Figs. 4 (a)-(d)). In Figs. 8 (a), (b) we compared our numerical results with the experimental data available in the search literature for low Reynolds numbers. One can see that at $Re = 150$, the present data and experimental data of Okajima [1] are in excellent agreement (Fig. 8 (a)). Furthermore, at $Re = 200$, the present numerical data are in good agreement with the experimental measurements of Okajima [1], Norberg [3] and Dutta et al. [4] (Fig. 8 (a)). The variation of C_{dmean} and C_d is almost same (Fig. 8 (a)). In addition, at $Re = 100$, we observed the excellent agreement between the present Strouhal number and those experimentally observed by Okajima [1] and Davis and Moore [2]. At $Re = 150$, again we observed reasonably good agreement between the present Strouhal number and experimentally examined by Norberg [3]. One can also see the good agreement between the present numerical data and experimental data at $Re = 200$ (Fig. 8 (b)). The Strouhal numbers either increase or decrease by increasing the Reynolds number. Norberg [3] observed similar trend for Strouhal number.

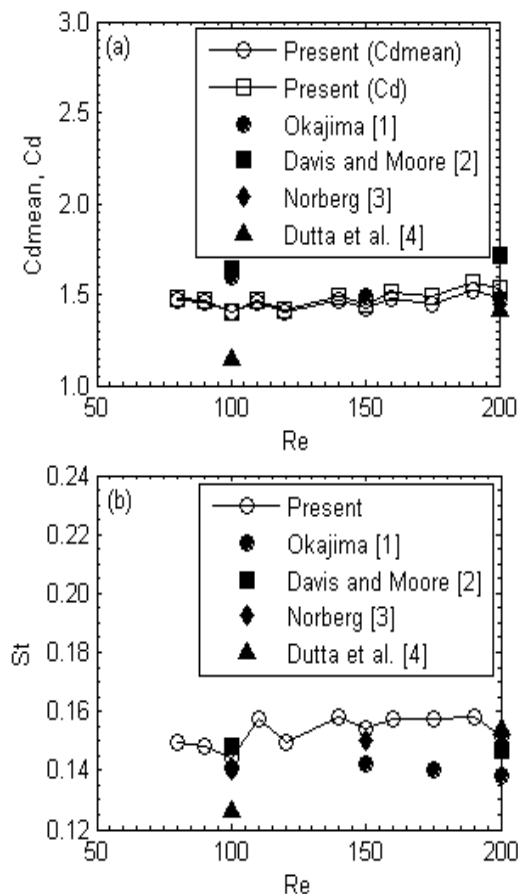
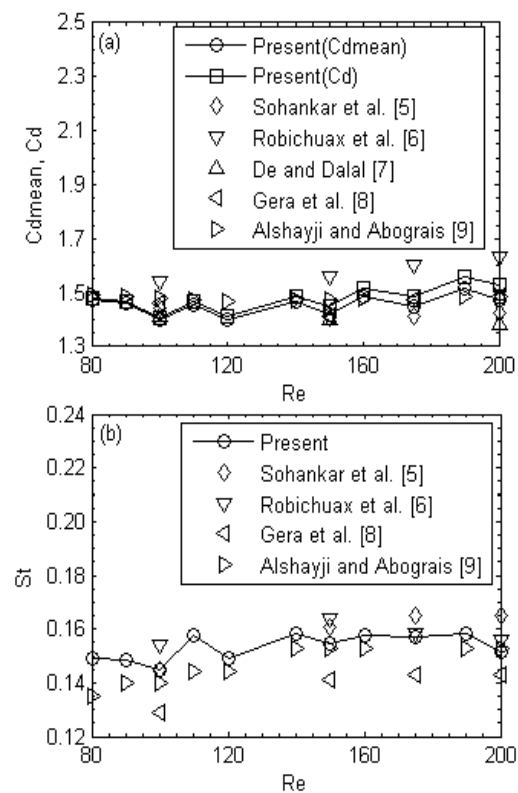


Fig. 8 (a), (b) Comparison of (a) C_{dmean} , C_d and (b) St of present data with the experimental data available in open literature

The calculation results for different Reynolds numbers for physical parameters are presented in Figs. 9 (a)-(d). For comparison, the numerical data available in the search literature are also presented in Figs. 9 (a)-(d). The results show that the physical parameters are affected up to some extent by the Reynolds numbers. The influence of Reynolds numbers is clearly seen on the Strouhal number, root-mean-square values of drag (C_{drms}) and lift (C_{lrms}) coefficients. As can be clearly seen the decreasing and increasing trend of the physical parameters with Reynolds number variation. The result of Sohanakr et al. [5], Gera et al. [8] and Alshyji and Abograis [9] lie closely on the present results for mean drag coefficient and drag coefficient (see Fig. 9 (a)). The results of Robichuax et al. [6] appear to be generally higher than those of all others. The present numerical results show that the mean drag coefficient and drag coefficient are slightly lower than those reported by Robichuax et al. [6] and Alshyji and Abograis [9] (see Fig. 9 (a)). Overall a good agreement between the present results and the open literature numerical data for mean drag coefficient and drag coefficient observed.

The Strouhal numbers are illustrated in Fig. 9 (b). The variation of St with Re shows a decreasing and increasing behaviour by increasing the Reynolds numbers (see Fig. 9 (b)). The excellent agreement observed between the present Strouhal numbers and those numerically observed by Alshyji and Abograis [9]. The present Strouhal number values are slightly higher than those observed by Gera et al. [8] numerically.



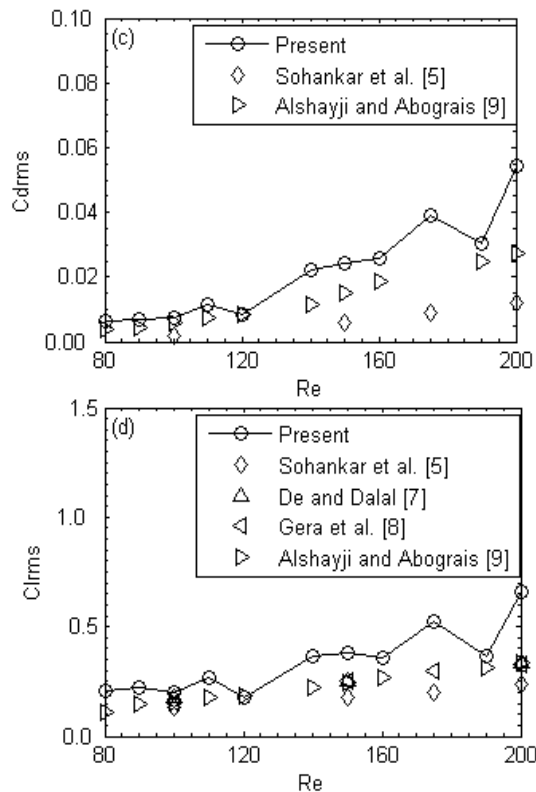


Fig. 9 (a)-(d) Comparison of (a) C_{dmean} , C_d , (b) St , (c) C_{drms} and (d) C_{lrms} of present data with the numerical data available in open literature

The root-mean-square values of drag and lift coefficients, C_{drms} and C_{lrms} are illustrated in Figs. 9 (c) and (d), respectively. Overall agreement between the present numerical data and those numerically observed by Sohankar et al. [5], De and Dalal [7], Gera et al. [8] and Alshayji and Abograis [9] (see Figs. 9 (c) and (d)). The present results are slightly higher than those observed numerically by other researchers.

III. CONCLUSIONS

A two-dimensional numerical study has been proposed in this paper to validate the code and to analyse some important flow features around a square cylinder for Reynolds numbers ranging from 80 to 200 using the multi-relaxation-time lattice Boltzmann method. We found that the vortex shedding is exhibited by a single primary frequency for all Reynolds numbers. The present study also predicted the influence of Reynolds numbers on physical quantities such as drag coefficient, mean drag coefficient, Strouhal number and root-mean-square values of drag and lift coefficients. The predicted numerical results for chosen computational domain show good trend with other experimental and numerical results. The satisfactory agreement we found between the present numerical data with the experimental results at low Reynolds numbers. The periodic natures for both drag and lift coefficients observed in this study. All these findings clearly show that the MRT-LBM is a good and suitable method for

bluff body flows. It is also found that by increasing the Reynolds numbers the physical parameters either increased or decreased.

REFERENCES

- [1] A. Okajima, "Strouhal numbers of rectangular cylinders," *Journal of Fluid Mechanics*, vol. ED-123, pp. 379-398, 1982.
- [2] R. W. Davis, and E. F. Moore, "A numerical study of vortex shedding from rectangles," *Journal of Fluid Mechanics*, vol. 116, pp. 475-506, 1982.
- [3] C. Norberg, "Flow around rectangular cylinders: Pressure forces and wake frequencies," *Journal of Wind Engineering and Industrial Aerodynamics*, vol. ED-40, pp. 187-196, 1993.
- [4] S. Dutta, P. K. Panigrahi, and K. Muralidhar, "Effect of orientation on the wake of a square cylinder at low Reynolds numbers," *Indian Journal of Engineering & Materials Sciences*, vol. 11, pp. 447-459, 2004.
- [5] A. Sohankar, L. Davidson, and C. Norberg, "Numerical simulation of unsteady flow around a square two-dimensional cylinder," *The Twelfth Australian Fluid Mechanics Conference, The University of Sydney, Australia*, pp. 517-520, 1995.
- [6] J. Robichaux, S. Balachandar, and S. P. Vanka, "Three-dimensional floquet instability of the wake of square cylinder," *Physics of Fluids*, vol. 1, pp. 560-578, 1999.
- [7] A. K. De, and A. Dalal, "Numerical simulation of unconfined flow past a triangular cylinder," *International Journal for Numerical Methods in Fluids*, vol. 52, pp. 801-821, 2006.
- [8] B. Gera, P. K. Sharma, and R. K. Singh, "CFD analysis of 2D unsteady flow around a square cylinder," *International Journal of Applied Engineering Research Dindigul*, vol. 1, pp. 602-610, 2010.
- [9] A. Alshayji, and A. Abograis, "Reduction of fluid forces on a square cylinder using passive control methods," *COMSOL Conference 2013, Boston, USA*.
- [10] S. Ul. Islam, H. Rahman, and W. S. Abbasi, "Grid independence study of flow past a square cylinder using the Multi-relaxation-time lattice Boltzmann method," *World Academy of Science, Engineering and Technology, International Journal of Mathematical, Computational, Physical and Quantum Engineering*, vol. 8, pp. 967-977, 2014.
- [11] U. Frisch, D. Hasslacher, and Y. Pomeau, "Lattice-gas automata for the Navier-Stokes equation," *Physical Review Letters*, vol. ED-56, pp. 1505-1508, 1986.
- [12] S. Ul. Islam, C. Y. Zhou, A. Shah, and P. Xie, "Numerical simulation of flow past rectangular cylinders with different aspect ratios using the incompressible lattice Boltzmann method," *Journal of Mechanical Science and Technology*, vol. 26, pp. 1027-1041, 2012.
- [13] S. Ul. Islam, C. Y. Zhou, and F. Ahmad, "Numerical simulations of cross-flow around four square cylinders in an in-line rectangular configuration," *World Academy of Science, Engineering and Technology*, vol. 3, pp. 780-789, 2009.
- [14] A. A. Mohamad, "Lattice Boltzmann Method: Fundamentals and Engineering Applications with Computer Codes," Springer, 2011.
- [15] I. Ginzburg, and D. d'Humieres, "Multireflection boundary conditions for lattice Boltzmann models," *Physical Review E*, vol. ED-68, pp.066614, 2003.
- [16] D. d'Humieres, "Generalized lattice Boltzmann equations. In Rarefied Gas Dynamics: Theory and Simulations," Shizgal BD, Weaver DP (eds). Progress in Astronautics and Aeronautics. Vol. 159. AIAA Press: Washington, DC, pp. 450-458, 1992.
- [17] S. Ul. Islam, and C. Y. Zhou, "Numerical simulation of flow around a row of circular cylinders using the Lattice Boltzmann method," *Information Technology Journal*, vol. ED-8, pp.513-520, 2009.
- [18] M. Cheng, D. S. Whyte, and J. Lou, "Numerical simulation of flow around a square cylinder in uniform shear flow," *Journal of Fluids and Structures*, vol. ED-23, pp. 207-226, 2007.
- [19] W. S. Abbasi, S. Ul. Islam, S. C. Saha, Y. T. Gu, and C. Y. Zhou, "Effect of Reynolds numbers on flow past four square cylinders in an in-line square configuration for different gap spacings," *Journal of Mechanical Science and Technology*, vol. ED-28, pp. 539-552, 2014.
- [20] Z. Guo, H. Liu, Li-S. Luo, and K. Xu, "A comparative study of the LBE and GKS methods for 2D near incompressible laminar flows," *Journal of Computational Physics*, vol. ED-227, pp. 4955-4976, 2008.
- [21] C. Rettinger, "Fluid flow simulations using the lattice Boltzmann method with multiple relaxation times, Friedrich-Alexander-Universitat

Erlangen-Nurnberg, Technische Fakultat. Department Informatik, Bachelor Thesis, 2013.

- [22] A. R. Rahmati, M. Ashrafizaadeh, and E. Shirani, "A multi-relaxation-time Lattice Boltzmann method on non-uniform grids for large eddy simulation of Rayleigh-Benard convection using two sub-grid scale models," *Journal of Applied Fluid Mechanics*, vol. ED-7, pp. 89-102, 2014.
- [23] D. P. Ziegler, "Boundary conditions for lattice Boltzmann simulations," *Journal of Statistical Physics*, vol. ED-71, pp.1171-1177, 1993.
- [24] Y. Dazchi, M. Renwei, L. S. Luo, and S. Wei, "Viscous flow computations with the method of lattice Boltzmann equation," *Progress in Aerospace Sciences*, vol. ED-39, pp. 329-367, 2003.